
Efficient Reasoning with Hidden Thinking

Xuan Shen¹ Yizhou Wang¹ Xiangxi Shi² Yanzhi Wang¹ Pu Zhao¹ Jiuxiang Gu³

Abstract

Chain-of-Thought (CoT) reasoning has become a powerful framework for improving complex problem-solving capabilities in Multimodal Large Language Models (MLLMs). However, the verbose nature of textual reasoning introduces significant inefficiencies. In this work, we propose **Heima** (as hidden llama), an efficient reasoning framework that leverages reasoning CoTs at hidden latent space. We design the Heima Encoder to condense each intermediate CoT into a compact, higher-level hidden representation using a single thinking token, effectively minimizing verbosity and reducing the overall number of tokens required during the reasoning process. Meanwhile, we design corresponding Heima Decoder with traditional Large Language Models (LLMs) to adaptively interpret the hidden representations into variable-length textual sequence, reconstructing reasoning processes that closely resemble the original CoTs. Experimental results across diverse reasoning MLLM benchmarks demonstrate that Heima model achieves higher generation efficiency while maintaining or even better zero-shot task accuracy. Moreover, the effective reconstruction of multimodal reasoning processes with Heima Decoder validates both the robustness and interpretability of our approach.

1. Introduction

The recent rise in popularity of Multimodal Large Language Models (MLLMs) (Dubey et al., 2024; Achiam et al., 2023; Bai et al., 2023; Liu et al., 2024b; Lai et al., 2024; Xu et al., 2024), which integrate vision techniques with traditional Large Language Models (LLMs), has spurred interest in leveraging Chain-of-Thought (CoT) (Wei et al., 2022) reasoning to enhance their capabilities for solving complex

problems. The CoT enables the MLLMs to generate intermediate steps that mirror human-like problem-solving processes, breaking down complex tasks into smaller, sequentially manageable components before arriving at the final solution. This approach not only enhances interpretability but also enables more effective multi-step reasoning, equipping MLLMs to address tasks that demand intricate logical understanding and contextual coherence, especially when processing the inherent complexity of visual information.

However, CoT reasoning often requires generating a substantial amount of additional text during the reasoning process, particularly for complex problems. This increased verbosity significantly impacts the efficiency of problem-solving, especially in large models with massive parameters and expensive inference costs. Thus, it becomes crucial to reduce the number of tokens generated during CoT reasoning to enhance the efficiency of MLLMs without compromising their reasoning capabilities.

Recent works (Hao et al., 2024; Deng et al., 2024b) have investigated compressing CoTs for GPT-2 (Radford & Wu, 2019), a relatively small language model compared to modern LLMs, which often consist of billions of parameters. The approach in (Hao et al., 2024) relies on task-specific fine-tuning for individual reasoning tasks, resulting in limited generalization. Moreover, these works focus solely on language-based tasks, leaving a substantial gap in compressing CoTs for large-scale multimodal models capable of handling diverse and intricate reasoning challenges.

Besides CoTs for LLMs, several works (Lai et al., 2024; Pi et al., 2023; Yan et al., 2024; Deng et al., 2024a) focus on enhancing reasoning in MLLMs using traditional visual decoders for segmentation, detection, and recognition, where the decoders are utilized to decode the input tokens generated by MLLMs. This demonstrates the effectiveness of MLLMs as encoders, motivating us for the further exploration of their role and mechanisms as encoders in the reasoning research area.

In this work, we propose Heima, the first efficient reasoning framework for MLLMs by leveraging reasoning CoTs in the hidden latent space, avoiding the reliance on verbose textual representations. We introduce the Heima Encoding method, which enables reasoning within the hidden space by encoding the CoTs into compact hidden repre-

¹Northeastern University ²Oregon State University ³Adobe Research. Correspondence to: Jiuxiang Gu <jigu@adobe.com>, Pu Zhao <p.zhao@northeastern.edu>.

Preprint version.

Code: <https://github.com/shawnricecake/Heima>

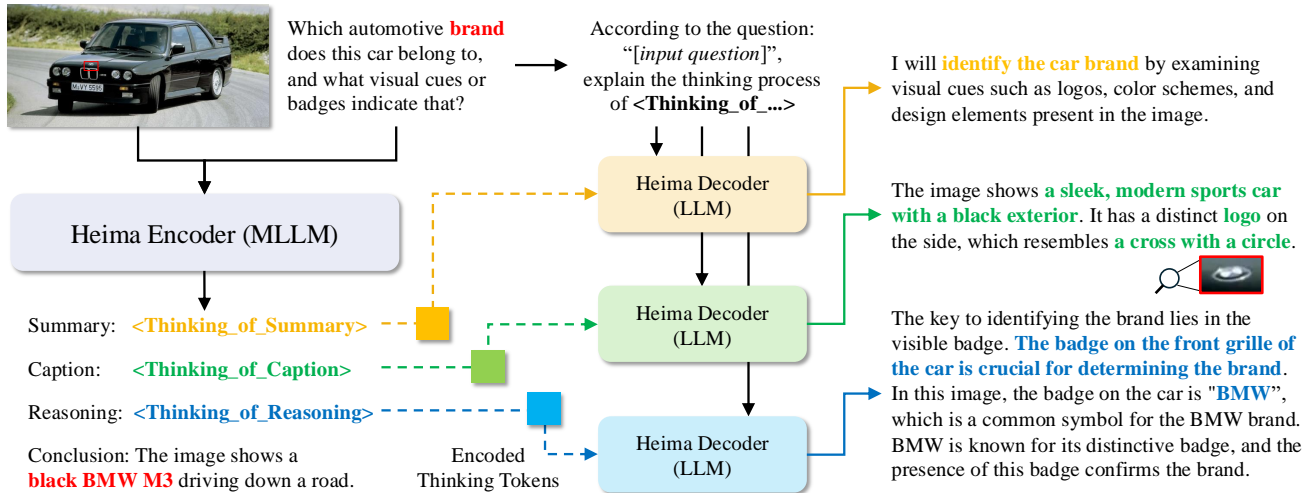


Figure 1. Visualization of our whole framework. Image and question are fed to the Heima Encoder (MLLM) for reasoning encoding and final conclusion generation. Encoded thinking tokens and question are then fed to the Heima Decoder (LLM) for the CoT reconstruction. In the reconstructed reasoning process, the caption decoder successfully retrieves image information, describing it as "The image shows a sleek, modern sports car with a black exterior" and identifying a distinct feature of the logo as "a cross with a circle." This demonstrates the effectiveness of the hidden representation encoded by the Heima Encoder, as the decoder, using only pure textual inputs, reconstructs the visual features. Furthermore, the reasoning decoder accurately deduces the logo as BMW based on this distinctive symbol.

sentations. Specifically, we train the reasoning MLLM as Heima Encoder to encode each CoT into a single thinking token, <CoT>, utilizing step-by-step encoding for more effective mapping. The the next-token prediction loss is preserved to constraint the Heima Encoder in generating the thinking tokens instead of verbose text during the reasoning process. Meanwhile, we propose the Heima Decoding method for adaptively decoding or interpreting the thinking tokens across varying context lengths. The traditional LLM is employed as the Heima Decoder for the reconstruction of hidden representations, guided by explanatory prompts.

The whole framework is shown in Figure 1. We accelerate the reasoning process using the Heima Encoder, which performs hidden thinking by generating (a significantly reduced number of) thinking tokens instead of textual CoTs, producing the final answer directly. The last hidden state of these thinking tokens can further be delivered to Heima Decoders for interpreting hidden thinking into a textual reasoning process. Experimental results demonstrate that our approach significantly enhances reasoning efficiency by generating far fewer tokens while achieving comparable or even superior performance on a list of zero-shot reasoning benchmarks, compared to reasoning MLLMs without hidden thinking. Furthermore, the results demonstrate that the reasoning processes reconstructed by the Heima Decoder, even without visual information, closely align with the original CoTs derived from both visual and textual inputs. This confirms both the effectiveness and interpretability of the hidden representations generated by the Heima Encoder. Meanwhile, existing efficient techniques like KV cache optimization

and flash attention are compatible with our method. Our contributions for this paper is summarized as follows,

- We propose Heima as the first reasoning acceleration framework for MLLMs through Heima Encoder by encoding the CoTs into compact hidden representations.
- We design Heima Decoder to decode or interpret hidden representations, validating the effectiveness of hidden thinking and enhancing interpretability.
- Experimental results demonstrate that our approach achieves high reasoning efficiency, reducing the number of generated tokens to as little as 6% of the original, while maintaining comparable or even superior performance on a list of zero-shot reasoning benchmarks compared to MLLMs utilizing textual CoTs.

2. Related Work

2.1. Chain-of-Thought Reasoning

With the theoretically validated effectiveness in recent works (Merrill & Sabharwal, 2023; Feng et al., 2024), CoTs have gained increasing popularity and are widely adopted as an enhancement method for generating intermediate reasoning processes before arriving at the final answer. The works (Wei et al., 2022; Khot et al., 2022; Zhou et al., 2022) focus on design the effective prompts which decompose the question into a group of reasoning steps for LLMs. The works (Yue et al., 2023; Yu et al., 2023; Wang et al., 2023;

Shao et al., 2024; Liu et al., 2024a) adopt additional fine-tuning to guide the model to generate reasoning chains. Meanwhile, to further enhance reasoning performance and make model reasoning more human-like, recent works (Xie et al., 2024; Gandhi et al., 2024; Su et al., 2024) have integrated additional search algorithms to improve the relevance of CoT generation to the input content. However, almost all of these works enhance reasoning performance by generating additional textual tokens, which incurs significant computational costs for large generative models with billions of parameters. This motivates us to explore the token reduction methods during the reasoning process.

2.2. Textual Efficient Reasoning

Recent works (Ning et al., 2023; Kou et al., 2024; Zhang et al., 2023; Li et al., 2024) aim to accelerate the reasoning process by employing parallel generation through templates or Jacobi decoding, which introduces additional overhead during model inference. Meanwhile, the works (Jiang et al., 2024; Ge et al., 2024; Chevalier et al., 2023; Qin et al., 2023; Liu et al., 2023; Munkhdalai et al., 2024) adopt contextual compression methods to achieve the efficient generation of the next following contexts based on the previous contexts. On the other hand, the work (Cheng & Van Durme, 2024) compresses the CoT into a short sequence of continuous embeddings for the acceleration of reasoning process. However, results on the math dataset reveal a significant degradation in accuracy, indicating the limitations and ineffectiveness of this approach. Thus, there is still a gap in developing efficient reasoning techniques for large models that maintain the performance advantages of reasoning with CoTs, which motivates us to explore better compression methods for CoTs to achieve higher accuracy and efficiency.

2.3. Reasoning in Latent Space

The works (Hao et al., 2024; Yang et al., 2024; Biran et al., 2024; Cheng & Van Durme, 2024) adopt latent reasoning for LLMs. For example, the work (Hao et al., 2024) addresses the compression of small models (GPT-2) on math datasets with CoTs. However, its effectiveness remains unverified as the evaluation of reasoning performance is limited to math datasets. Additionally, the small model size raises concerns about potential overfitting to the data rather than general reasoning based on the inputs.

Some works (Liu et al., 2024b; Lai et al., 2024) include visual information into latent space for MLLMs to enhance the textual reasoning. The work (Lai et al., 2024) employs fine-tuning for both LLMs and segmentation decoders, demonstrating the potential to decode visual information in tokens generated by LLMs. Specifically, this approach leverages segment tokens generated by MLLMs as part of the input for the segmentation decoder, emphasizing their utility in

enhancing the decoding process. Nevertheless, subsequent works (Pi et al., 2023; Deng et al., 2024a; Yan et al., 2024) continue to investigate using MLLMs to generate tokens for visual downstream tasks, rather than exploring the construction of internal feature representations within MLLMs for higher-level feature embedding. The absence of feature construction in MLLMs motivates us to explore the development of latent representations for these models.

3. Methodology

In this section, we first present the CoT encoding process, which encodes CoTs into compact hidden representations. Then, we detail the adaptive decoding process, which reconstructs or interprets the hidden representations into CoT-like trajectories. Finally, we explain for the efficient reasoning with the proposed hidden thinking.

3.1. Design of Heima Encoder

Heima Encoder encodes verbose textual CoTs into compact hidden representations with very few tokens, thus accelerating the CoT Reasoning with higher efficiency.

CoT Encoding. The original CoT training dataset can be defined as

$$\{(X_v^{(i)}, X_q^{(i)}, \{\text{CoT}_{(k)}^{(i)}\}_{k=1}^{K_i}, Y_a^{(i)})\}_{i=1}^N, \quad (1)$$

where $X_v^{(i)}$ denotes the i^{th} visual input, $X_q^{(i)}$ denotes the i^{th} query input, $\{\text{CoT}_{(k)}^{(i)}\}_{k=1}^{K_i}$ denotes that there are K_i stages for the textual CoT sentence with $\text{CoT}_{(k)}^{(i)}$ as the k^{th} CoT stage in the i^{th} data sample, and $Y_a^{(i)}$ denotes the final answer. For example, as shown in Figure 1, the CoT has Summary, Caption, and Reasoning stages.

We first adopt the pretrained MLLM as the initialization of Heima Encoder $f_{\theta}(\cdot)$, where θ denotes its parameters, and fine-tune it to learn to generate the answer $Y_a^{(i)}$ with $\{\text{CoT}_{(k)}^{(i)}\}_{k=1}^{K_i}$, conditioned on both image $X_v^{(i)}$ and textual query $X_q^{(i)}$ as follows,

$$\max_{\theta} \frac{1}{N} \sum_{i=1}^N \log P_{\theta}(\{\text{CoT}_{(k)}^{(i)}\}_{k=1}^{K_i}, Y_a^{(i)} | X_v^{(i)}, X_q^{(i)}). \quad (2)$$

After training on explicit CoTs, we then update the training set by replacing each $\text{CoT}_{(k)}^{(i)}$ with a single thinking token—denoted as $\langle \text{CoT} \rangle_{(k)}$. For each thinking token $\langle \text{CoT} \rangle_{(k)}$ at the k^{th} stage, it is defined with a unique special token and added to the vocabulary to enable explicit textual visualization of the reasoning process. For example, in Figure 1, we define a token $\langle \text{Thinking_of_Summary} \rangle$ as the thinking token for the summary stage. Similarly, we define $\langle \text{Thinking_of_Caption} \rangle$ for the caption stage and

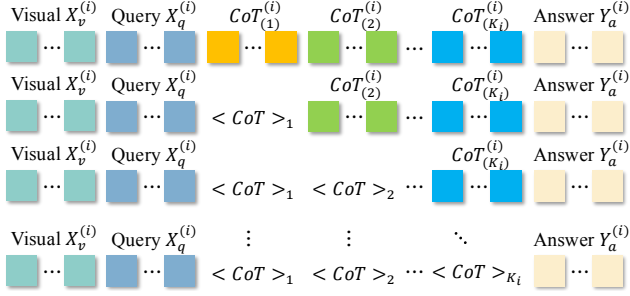


Figure 2. Visualization of the CoTs progressive encoding process.

`<Thinking_of_Reasoning>` for the reasoning stage. Note that different samples with varying values of i share the same thinking token $\langle \text{CoT} \rangle_{(k)}$ at the same stage k . The updated dataset is then explained as follows,

$$\left\{ (X_v^{(i)}, X_q^{(i)}, \{\langle \text{CoT} \rangle_{(k)}\}_{k=1}^{K_i}, Y_a^{(i)}) \right\}_{i=1}^N. \quad (3)$$

We then continue fine-tuning the model with the objective:

$$\max_{\theta} \frac{1}{N} \sum_{i=1}^N \log P_{\theta} \left(\{\langle \text{CoT} \rangle_{(k)}\}_{k=1}^{K_i}, Y_a^{(i)} \mid X_v^{(i)}, X_q^{(i)} \right). \quad (4)$$

Through this fine-tuning process, we guide the model to encode intermediate CoTs into hidden representations within the thinking tokens, prompting the MLLM to perform reasoning without producing verbose textual CoTs. Meanwhile, through the next-token prediction constraint, the explicit textual symbols of the hidden representations for Heima Encoder are aligned to the text of the corresponding special tokens $\{\langle \text{CoT} \rangle_{(k)}\}_{k=1}^{K_i}$ in vocabulary, while the hidden representations contained in hidden states of thinking tokens remain distinct and variable depending on the inputs.

Progressive Encoding. To facilitate a seamless transition from textual reasoning to hidden thinking while maintaining model performance, we adopt a progressive encoding strategy as shown in Figure 2. Specifically, there are multiple CoT stages and we do not encode all of the CoT stages into hidden representations at the start of the training. Instead, during training, we gradually increase the number of CoT stages with hidden representations, from 0 to $\max\{K_i\}_{i=1}^N$. Specifically, starting from 0 stages without hidden representations, we train the model using textual $\{\text{CoT}_{(k)}^{(i)}\}_{k=1}^{K_i}$ without any thinking tokens following Equation (2) for a few training steps. Then we encode one CoT stage into a single thinking token and train for a few steps. Next, two CoT stages (including the previous trained CoT stage) are trained with their corresponding thinking tokens. Subsequently, we continue to add more CoT stages into the thinking token training for Heima Encoder θ and finally all CoT stages are trained with thinking tokens for hidden representations.

Formally, our progressive encoding has $\max\{K_i\}_{i=1}^N + 1$ stages. In the s^{th} stage ($s \in \mathbb{N}, 0 \leq s \leq \max\{K_i\}_{i=1}^N$), we prepare the training data as

$$\left\{ (X_v^{(i)}, X_q^{(i)}, \{\langle \text{CoT} \rangle_{(k)}\}_{k=1}^s, \{\text{CoT}_{(k)}^{(i)}\}_{k=s+1}^{K_i}, Y_a^{(i)}) \right\}_{i=1}^N. \quad (5)$$

For $s = 0$, the model is fine-tuned following Equation (2). In the s^{th} stage ($s > 0$), we finetune Heima Encoder $f_{\theta}(\cdot)$,

$$\max_{\theta} \frac{1}{N} \sum_{i=1}^N \log P_{\theta} \left(\{\langle \text{CoT} \rangle_{(k)}\}_{k=1}^s, \{\text{CoT}_{(k)}^{(i)}\}_{k=s+1}^{K_i}, Y_a^{(i)} \mid X_v^{(i)}, X_q^{(i)} \right). \quad (6)$$

In the above expression, during the s^{th} stage encoding, the first s CoT stages are trained with hidden thinking tokens while the rest CoT stages are trained with textual reasoning tokens. As the value of s increases, more CoT stages are encoded into hidden representations. It is illustrated in Figure 2 with each row representing the training data of one stage in the training.

This approach allows the model to gradually internalize the reasoning processes represented by multiple CoTs and integrate them into its hidden representations. After the final progressive stage, we further optimize the hidden representations of the thinking tokens by performing one additional recovering stage, which continue to train the model following Equation (6) with $s = \max\{K_i\}_{i=1}^N$ (i.e., Equation (4)) for a few more training steps. This extra recovering stage optimizes the transitions and interactions between the hidden representations across different stages, ensuring a cohesive alignment of information learned throughout the encoding process. Additionally, it consolidates the overall learning process, enhancing the model’s ability to effectively utilize the encoded reasoning patterns for improved performance and robustness in downstream reasoning tasks.

3.2. Design of Heima Decoder

After each CoT stage has been encoded into a single thinking token and stored in the hidden representation, it is necessary to recover the textual reasoning process for interpretability and analysis, enabling better utilization in practice. Meanwhile, it is crucial to verify the effectiveness of the hidden representations encapsulated within thinking tokens to ensure that the model is genuinely learning hidden reasoning processes rather than merely fitting the data. Thus, to interpret the thinking tokens, we design the adaptive Heima Decoder, which exploits the standard next-token prediction paradigm in LLMs for the reconstruction of variable-length (i.e., adaptive) textual sequence based on thinking tokens.

Adaptive Decoding. After Heima Encoder, a total of $\max\{K_i\}_{i=1}^N$ CoT stages are encoded into hidden repre-

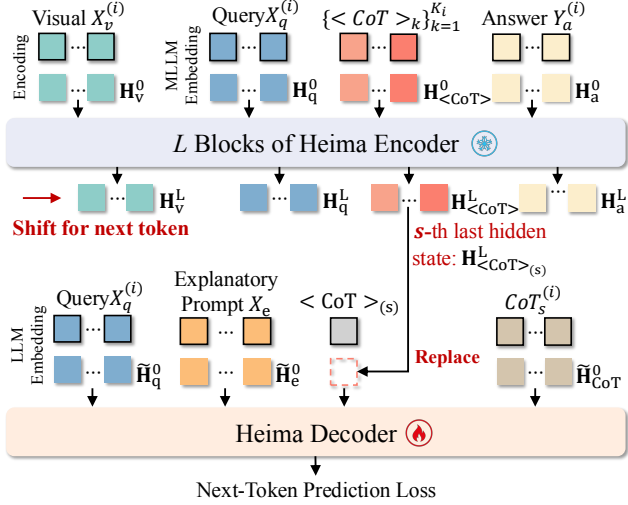


Figure 3. Visualization of the training progress for Heima Decoder. Thinking token is caught from the s^{th} last hidden state of Heima Encoder and replaces the embedding of special token $\langle CoT \rangle_{(s)}$.

sentations, each with a unique thinking token. Each encoded CoT stage or each kind of thinking token requires one corresponding decoder or interpreter. Thus, to decode multiple thinking tokens, we need to train multiple decoders separately, following the same procedure as below.

We adopt a pretrained LLM as the initialization of Heima Decoder $f_{\eta_s}(\cdot)$ for the s^{th} stage encoded with the s^{th} thinking token ($s \in \mathbb{N}, 1 \leq s \leq \max\{K_i\}_{i=1}^N$), where η_s denotes its parameters. We do not consider the case of $s = 0$ as it does not include thinking tokens. The training dataset for Heima Decoder of the s^{th} stage is designed as follows,

$$\{(X_e, X_q^{(i)}, \langle CoT \rangle_{(s)}, H_{\langle CoT \rangle_{(s)}}^{(i)}, CoT_{(s)}^{(i)})\}_{i=1}^N, \quad (7)$$

where X_e denotes the explanatory prompts to guide the model for the interpretation of the thinking tokens. $X_q^{(i)}$ denotes the i^{th} query. $\langle CoT \rangle_{(s)}$ denotes the s^{th} thinking token, and $H_{\langle CoT \rangle_{(s)}}^{(i)}$ denotes the hidden representation (last hidden states) of the thinking token $\langle CoT \rangle_{(s)}$ encoded by Heima Encoder with $\{X_v^{(i)}, X_q^{(i)}, \{\langle CoT \rangle_{(k)}\}_{k=1}^{K_i}, Y_a^{(i)}\}$. $CoT_{(s)}^{(i)}$ denotes the s^{th} textual CoT in the i^{th} sample. Note that here we only use LLMs as the decoders without the capability to read images, and the dataset for training decoders only has text queries without visual images inputs.

During the fine-tuning of Heima Decoder, the frozen Heima Encoder is used to generate the thinking tokens as inputs for decoders. Specifically, for the thinking token inputs, we use the last hidden states of the thinking tokens from Heima Encoder, i.e., $H_{\langle CoT \rangle_{(s)}}^{(i)}$, to replace the position previously occupied by the thinking token symbol $\langle CoT \rangle_{(s)}$ after the word embedding in Heima Decoder, as illustrated in Figure 3. The next-token prediction loss is remained and Heima

Decoder is fine-tuned as follows,

$$\max_{\eta_s} \frac{1}{N} \sum_{i=1}^N \log P_{\eta_s} (CoT_{(s)}^{(i)} | X_e, X_q^{(i)}, H_{\langle CoT \rangle_{(s)}}^{(i)}), \quad (8)$$

During the finetuning of the decoder, note that we do not directly use the thinking token $\langle CoT \rangle_{(s)}$ as input. Instead, we use the last hidden state $H_{\langle CoT \rangle_{(s)}}^{(i)}$ from Heima Encoder as part of inputs for Heima decoder, since the reasoning information are actually encapsulated in the last hidden state of the thinking token rather than the textual symbol.

Explanatory Prompts. A single hidden representation $H_{\langle CoT \rangle_{(s)}}^{(i)}$ alone is insufficient to guide Heima Decoder $f_{\eta_s}(\cdot)$ toward reconstructing the original reasoning stages, as language models generally rely on textual instructions to scaffold the generation process. Thus, we provide the explanatory prompt for Heima Decoder to enhance usability and interpretability. We use the following prompt,

“According to the question: $[X_q^{(i)}]$, can you explain the thinking progress of $\langle CoT \rangle_{(s)}$?”

These explanatory prompts ensure that the output reasoning process remains (i) aligned with the original query $[X_q^{(i)}]$ and (ii) consistent with the hidden reasoning encoded by Heima Encoder. More formally, the prompt provides extra text X_e that conditions the decoding distribution as follows,

$$\begin{aligned} & P_{\eta_s} (CoT_{(s)}^{(i)} | X_e, X_q^{(i)}, H_{\langle CoT \rangle_{(s)}}^{(i)}) \\ &= \prod_{t=1}^{T_{(s)}^{(i)}} P_{\eta_s} (w_t^{(s,i)} | w_{<t}^{(s,i)}, X_q^{(i)}, X_e, H_{\langle CoT \rangle_{(s)}}^{(i)}), \quad (9) \end{aligned}$$

where $t \in \mathbb{N}, 1 \leq t \leq T_{(s)}^{(i)}$, $T_{(s)}^{(i)}$ denotes the token length of $CoT_{(s)}^{(i)}$, and $w_t^{(s,i)}$ denote the t -th token of $CoT_{(s)}^{(i)}$. This textual scaffolding guides the LLM based Heima Decoder to leverage the explicit question context $X_q^{(i)}$, to interpret and explain the hidden representations, encapsulated in the last hidden states $H_{\langle CoT \rangle_{(s)}}^{(i)}$, with textual reasoning processes during hidden thinking.

3.3. Efficient Reasoning

To achieve the acceleration during the reasoning process with our framework, we first deploy Heima Encoder only as the reasoning model, ensuring lower memory requirements and faster generation. Heima Encoder generates the response corresponding to the input question and image as follows,

$$\begin{aligned} & P_{\theta} (\{\langle CoT \rangle_{(k)}\}_{k=1}^{K_i}, Y_a^{(i)} | X_v^{(i)}, X_q^{(i)}) \\ &= \prod_{t=1}^{T^{(i)}+K_i} P_{\theta} (w_t^{(i)} | w_{<t}^{(i)}, X_v^{(i)}, X_q^{(i)}), \quad (10) \end{aligned}$$

Table 1. Main results compared to Llama3.2-11B-Vision-Instruct and LLaVA-CoT with both accuracy and number of generated tokens on 6 different multimodal reasoning benchmarks.

Dataset	MMSar	MMBench	MMVet	MathVista	AI2D	Hallusion	Average
Model	Acc. / # Token	Acc.					
Llama3.2-11B Vision-Instruct	48.1 (140.0)	58.2 (64.7)	50.2 (106.0)	50.3 (240.1)	68.5 (74.9)	37.2 (91.4)	52.1
LLaVA-CoT	54.0 (181.0)	70.7 (154.8)	49.8 (227.2)	50.9 (216.3)	77.6 (178.5)	63.8 (177.9)	61.1
Heima w/o progressive	49.7 (13.1)	72.5 (13.3)	39.0 (71.7)	39.3 (13.6)	75.9 (12.6)	61.3 (15.6)	56.3
Heima w/o recover	49.8 (13.0)	71.6 (13.2)	42.8 (79.6)	39.8 (14.0)	77.3 (12.7)	58.5 (17.5)	56.6
Heima	49.9 (12.8)	72.8 (12.9)	43.3 (75.8)	43.6 (13.8)	77.5 (12.7)	60.6 (16.9)	58.0

where $(w_1^{(i)}, w_2^{(i)}, \dots, w_{K_i}^{(i)})$ denotes the chain of thinking tokens for hidden thinking, and the $Y_a^{(i)} = (w_{K_i+1}^{(i)}, w_{K_i+2}^{(i)}, \dots, w_{K_i+T(i)}^{(i)})$ denotes the chain of tokens corresponding to the final answer. Thus, we obtain the final answer faster with Heima Encoder through hidden thinking with K_i tokens, avoiding the need of complex and verbose CoTs that require generating a significantly larger number of tokens $\sum_{k=1}^{K_i} |\text{CoT}_{(k)}^{(i)}|$. Additionally, the last hidden states of the thinking tokens, encapsulating the hidden thinking process, can be saved offline for future interpretation into an explicit textual reasoning process with Equation (9).

4. Experimental Results

4.1. Experiment Setup

Dataset. We utilize the LLaVA-CoT-100k dataset, a reasoning dataset for MLLMs that integrates samples from several widely used VQA datasets. It comprises 100k image-QA pairs with three stages of CoT reasoning: summary, caption, and reasoning.

Model Training. We adopt the LLaVA-CoT (Xu et al., 2024) pretrained model based on Llama-3.2-11B-Vision-Instruct (Meta, 2024b) as our initialization of Heima Encoder. Meanwhile, Llama-3.1-8B-Instruct (Meta, 2024a) is employed as the initialization of Heima Decoder. We use torchtune (Meta, 2024c) as the model training framework with LoRA (Hu et al., 2021) for both Heima Encoder and Heima Decoder. During the progressive encoding process, we freeze the image encoder component and fine-tune both the decoder and fusion components of the LLaVA-CoT model. This fine-tuning includes the entire attention and MLP modules across all layers, as well as the output projection layer, using a rank of 16, and an alpha of 32. As for training Heima Decoder, we apply the same lora setting to the model. Detailed hyperparameters are included in Appendix A. The training is conducted on $8 \times$ H100 GPUs.

Evaluation. We adopt several challenging zero-shot benchmarks to verify the effectiveness of our proposed method, including MMStar (Chen et al., 2024), MMBench V1.1 (Liu et al., 2025), MMVet (Yu et al., 2024), MathVista (Lu et al., 2024), AI2D (Hiippala et al., 2021), and HallusionBench (Guan et al., 2024). MMStar, MMBench, and MMVet evaluate general visual question-answering capabilities, while MathVista and AI2D assess mathematical and scientific reasoning. HallusionBench, in contrast, targets language hallucinations and visual illusions. We use the VLMEvalKit (Duan et al., 2024) as the evaluation pipeline to ensure a fair comparison. We use GPT-4o (Achiam et al., 2023) for evaluation on the MMVet and MathVista datasets, while exact match evaluation is applied to other datasets using VLMEvalKit. For Heima Decoder, we split the LLaVA-CoT-100k dataset for train and test separately. We evaluate the fine-tuned Heima Decoder on test set which contain 4300 samples with metrics including BLEU-4 (Papineni et al., 2002), METEOR (Banerjee & Lavie, 2005), ROUGE (Lin, 2004), and BERTScore (Zhang et al., 2019). Additionally, we adopt GPT-4o for the similarity analysis.

4.2. Main Results

We first provide the main results for Heima Encoder in Table 1. We compare our method to the original Llama3.1-11B-Vision-Instruct model and the LLaVA-CoT on 6 datasets for the evaluation of zero-shot performance. Heima outperforms the Llama3.1-11B-Vision-Instruct model in both accuracy and performance while utilizing significantly fewer tokens, particularly on benchmarks such as MMBench, AI2D, and Hallusion. Compared to the baseline model LLaVA-CoT, Heima retains most of the model’s performance while requiring as little as 6% of the tokens on certain datasets. Notably, on MMBench, Heima achieves better accuracy than the baseline LLaVA-CoT. Furthermore, to evaluate the effectiveness of progressive encoding, we include accuracy results using one-shot encoding to encode all CoT stages through the whole training (i.e., non-progressive

Table 2. MathVista detailed results. SC denotes scientific reasoning, TQA denotes textbook question answering, NC denotes numeric commonsense, AC denotes arithmetic reasoning, VQA denotes visual question answering, GR denotes geometry reasoning, AR denotes algebraic reasoning, GPS denotes geometry problem solving, MWP denotes math word problem, LR denotes logical reasoning, FQA denotes figure question answering, SR denotes statistical reasoning. Overall accuracy is a weighted metric based on sample counts.

Model	SC	TQA	NC	AC	VQA	GR	AR	GPS	MWP	LR	FQA	SR	Overall Acc.	# Token
Llama3.2-11B Vision-Instruct	62.3	60.1	31.3	43.3	35.2	47.3	46.3	46.6	55.4	18.9	53.9	65.1	50.3	240.1
LLaVA-CoT	57.4	57.0	33.3	44.5	43.0	54.8	54.1	56.7	47.8	8.1	50.2	60.8	50.9	216.3
Heima w/o progressive	58.2	51.9	27.8	32.3	34.1	31.4	32.7	31.7	33.9	16.2	45.0	46.8	39.3	13.6
Heima w/o recover	58.2	53.8	30.6	34.3	34.6	29.3	31.0	27.4	41.9	21.6	43.1	44.2	39.8	14.0
Heima	54.9	55.1	32.6	36.0	36.3	41.0	42.3	40.9	44.1	10.8	43.5	45.2	43.6	13.8

Table 3. MMStar detailed results. CP denotes coarse perception, FP denotes fine-grained perception, IR denotes instance reasoning, LR denotes logical reasoning, S&T denotes Science&Technology.

Model	CP	FP	IR	LR	Math	S & T
Llama3.2-11B Vision-Instruct	64.0	39.2	53.6	51.6	51.6	28.4
LLaVA-CoT	66.0	40.0	64.4	52.4	60.8	40.4
Heima w/o progressive	66.0	43.2	62.4	45.6	44.8	36.0
Heima w/o recover	64.8	44.0	57.2	51.6	44.0	37.2
Heima	62.0	43.2	58.8	52.8	48.0	34.8

encoding). The results indicate that the non-progressive Heima Encoder performs worse, confirming the advantage and effectiveness of the progressive encoding approach. Additionally, the accuracy results without the recovering stage highlight its necessity, as they demonstrate a noticeable decline in performance compared to that with the recovering stage after completing the encoding of all CoT stages.

To further investigate the model’s performance across different types of reasoning problems, we present detailed accuracy results for various classifications of reasoning tasks in MathVista and MMStar, as shown in Table 2 and Table 3, respectively. In MathVista, the model retains most of its accuracy across geometry reasoning (GR), algebraic reasoning (AR), geometry problem solving (GPS), and math word problems (MWP), demonstrating that both progressive encoding and recovering enhance the preservation of reasoning capabilities for mathematical problems. Meanwhile, in MMStar, Heima outperforms Llama3.2-11B on both instance reasoning (IR) and logical reasoning (LR) tasks while using less than 10% of the tokens, and it preserves the majority of its reasoning capabilities for mathematical problems through progressive encoding.

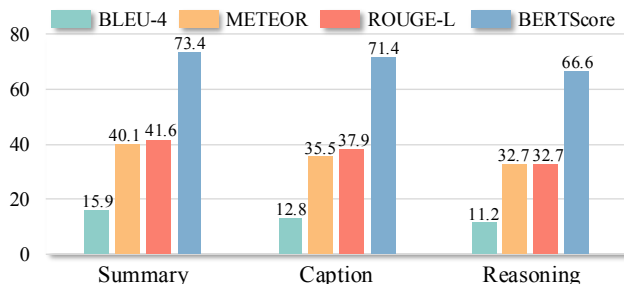


Figure 4. Results of BLEU-4, METEOR, GROUGE-L, and BERTScore for 3 decoders.



Figure 5. Results of evaluation by GPT-4o for assessing the average similarity score (1-5) between the reconstructed reasoning processes from the thinking tokens and the original CoTs.

4.3. Interpretability Analysis

To verify the effectiveness of hidden representation encoding and improve interpretability of the framework, we evaluate the performance of Heima Decoder by assessing the similarity between the reconstructed reasoning process and the ground-truth CoT. We provide the results of 4 evaluation metrics in Figure 4, and the detailed results are included in Table A2 of Appendix B. The reconstruction is most successful for the summary stage, followed by the caption stage, and then the reasoning stage. This is primarily because the summary stage relies mainly on the input question, while both the caption and reasoning stages require detailed and comprehensive visual information for accurate reasoning.

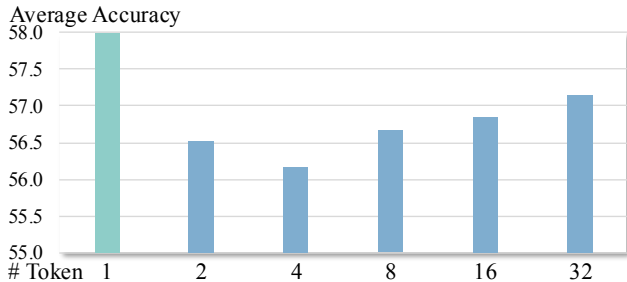


Figure 6. Ablation study of zero-shot performance on 6 datasets for different number of thinking tokens for each CoT.

Notably, as shown in Figure 1, Heima Decoder uses LLMs without visual inputs, yet it reconstructs reasoning processes with key visual features, validating that the thinking tokens encode visual features in hidden representations.

Furthermore, we adopt GPT-4o to evaluate the similarity between the reconstructed reasoning process and the original CoTs, with the results presented in Figure 5. We treat the evaluation as a ranking process to classify the performance of reconstructed reasoning process into 5 ranks, from 1 to 5. Rank 1 represents the reconstructed reasoning process and ground-truth CoT describes different themes and has little overlapping in between, while Rank 5 represents the reconstruction well aligned with the ground truth. We remove special tokens in both sides and input them to GPT-4o to rank the similarity for each stage. We also include corresponding image-question pairs in the prompt as additional reference for more accurate context support. The detailed prompts provided for GPT-4o are included in Appendix C. We average the rank of all samples in one stage to estimate the similarity score of the stage. The results demonstrate that all three stages are effectively reconstructed by our Heima Decoder, with particularly strong performance in the summary stage, which primarily relies on textual information. Notably, the score of the reasoning stage excels that of the caption stage. The reasoning stage requires the integration of both textual and visual information, showcasing the robustness and versatility of our proposed framework.

4.4. Ablation Study

We explore the performance with different number of thinking tokens for each CoT. We provide this ablation study on 6 datasets in Figure 6 with details in Table A3 of Appendix B. The results show that one single token for encoding the corresponding CoT achieves the best performance.

Additionally, we investigate adaptive encoding by regulating the retention ratio of thinking tokens, where the number of thinking tokens is determined as a percentage of the original CoT token length. We provide the results in Figure 7 with details in Table A4 of Appendix B. As observed, from 10%

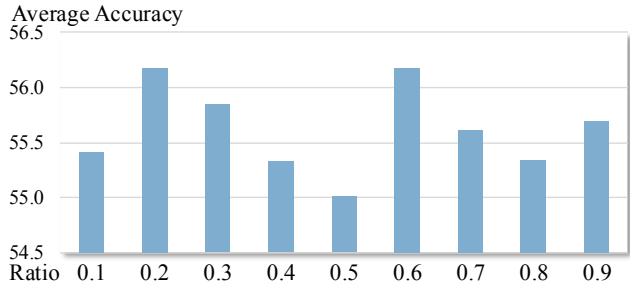


Figure 7. Ablation study of average accuracy on 6 datasets for varying retention ratios of thinking tokens relative to original CoT.

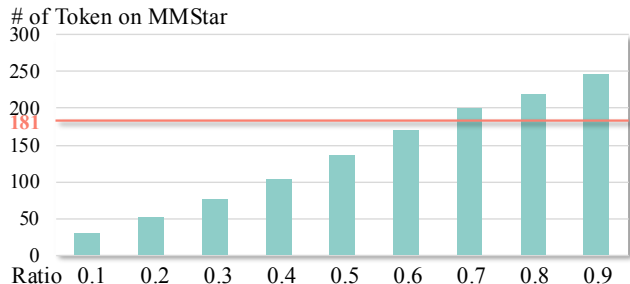


Figure 8. Ablation study for number of generated tokens on MMStar with varying retention ratios of thinking tokens relative to the original CoT. Baseline (i.e., LLaVA-CoT) generates 181 tokens.

to 90% retention ratio, accuracy fluctuates irregularly. There is no consistent pattern emerging, highlighting the unpredictable relationship between retention ratio and accuracy. Meanwhile, as shown in Figure 8, the number of generated token is continuously increasing as the retention ratio becomes large. Notably, when the retention ratio reaches 70%, the number of generated tokens exceeds that of the baseline model (i.e., LLaVA-CoT), further indicating that adaptive encoding is not an effective method for generally capturing the features of the reasoning process.

5. Conclusion

In this paper, we propose Heima for efficient reasoning with hidden thinking. We fine-tune Heima Encoder by encoding each CoT into a single token, and Heima Decoder is fine-tuned by incorporating explanatory prompts to decode the hidden representations encapsulated within the thinking tokens. By effectively reconstructing the reasoning process through Heima Decoder, we demonstrate the robustness and interpretability of our method. Experimental results show that our method achieves comparable or even better accuracy on zero-shot benchmarks with significantly fewer tokens, highlighting the efficiency and reliability. In future research, we plan to extend our method to larger models for Heima Encoder and explore the use of smaller LLMs as Heima Decoder to support diverse scale designs.

Impact Statement

This paper presents work whose goal is to advance the field of Machine Learning. There are many potential societal consequences of our work, none which we feel must be specifically highlighted here.

References

- Achiam, J., Adler, S., Agarwal, S., Ahmad, L., Akkaya, I., Aleman, F. L., Almeida, D., Altenschmidt, J., Altman, S., Anadkat, S., et al. Gpt-4 technical report. *arXiv preprint arXiv:2303.08774*, 2023.
- Bai, J., Bai, S., Yang, S., Wang, S., Tan, S., Wang, P., Lin, J., Zhou, C., and Zhou, J. Qwen-vl: A versatile vision-language model for understanding, localization, text reading, and beyond. *arXiv preprint arXiv:2308.12966*, 2023.
- Banerjee, S. and Lavie, A. Meteor: An automatic metric for mt evaluation with improved correlation with human judgments. In *Proceedings of the acl workshop on intrinsic and extrinsic evaluation measures for machine translation and/or summarization*, pp. 65–72, 2005.
- Biran, E., Gottesman, D., Yang, S., Geva, M., and Globerson, A. Hopping too late: Exploring the limitations of large language models on multi-hop queries. *arXiv preprint arXiv:2406.12775*, 2024.
- Chen, L., Li, J., Dong, X., Zhang, P., Zang, Y., Chen, Z., Duan, H., Wang, J., Qiao, Y., Lin, D., et al. Are we on the right way for evaluating large vision-language models? *arXiv preprint arXiv:2403.20330*, 2024.
- Cheng, J. and Van Durme, B. Compressed chain of thought: Efficient reasoning through dense representations. *arXiv preprint arXiv:2412.13171*, 2024.
- Chevalier, A., Wettig, A., Ajith, A., and Chen, D. Adapting language models to compress contexts. *arXiv preprint arXiv:2305.14788*, 2023.
- Deng, A., Chen, T., Yu, S., Yang, T., Spencer, L., Tian, Y., Mian, A. S., Bansal, M., and Chen, C. Motion-grounded video reasoning: Understanding and perceiving motion at pixel level. *arXiv preprint arXiv:2411.09921*, 2024a.
- Deng, Y., Choi, Y., and Shieber, S. From explicit cot to implicit cot: Learning to internalize cot step by step. *arXiv preprint arXiv:2405.14838*, 2024b.
- Duan, H., Yang, J., Qiao, Y., Fang, X., Chen, L., Liu, Y., Dong, X., Zang, Y., Zhang, P., Wang, J., et al. Vlmevalkit: An open-source toolkit for evaluating large multi-modality models. In *Proceedings of the 32nd ACM International Conference on Multimedia*, pp. 11198–11201, 2024.
- Dubey, A., Jauhri, A., Pandey, A., Kadian, A., Al-Dahle, A., Letman, A., Mathur, A., Schelten, A., Yang, A., Fan, A., et al. The llama 3 herd of models. *arXiv preprint arXiv:2407.21783*, 2024.
- Feng, G., Zhang, B., Gu, Y., Ye, H., He, D., and Wang, L. Towards revealing the mystery behind chain of thought: a theoretical perspective. *Advances in Neural Information Processing Systems*, 36, 2024.
- Gandhi, K., Lee, D., Grand, G., Liu, M., Cheng, W., Sharma, A., and Goodman, N. D. Stream of search (sos): Learning to search in language. *arXiv preprint arXiv:2404.03683*, 2024.
- Ge, T., Jing, H., Wang, L., Wang, X., Chen, S.-Q., and Wei, F. In-context autoencoder for context compression in a large language model. In *The Twelfth International Conference on Learning Representations*, 2024. URL <https://openreview.net/forum?id=uREj4ZuGJE>.
- Guan, T., Liu, F., Wu, X., Xian, R., Li, Z., Liu, X., Wang, X., Chen, L., Huang, F., Yacoob, Y., Manocha, D., and Zhou, T. Hallusionbench: An advanced diagnostic suite for entangled language hallucination and visual illusion in large vision-language models. In *Proceedings of the IEEE/CVF Conference on Computer Vision and Pattern Recognition (CVPR)*, pp. 14375–14385, June 2024.
- Hao, S., Sukhbaatar, S., Su, D., Li, X., Hu, Z., Weston, J., and Tian, Y. Training large language models to reason in a continuous latent space. *arXiv preprint arXiv:2412.06769*, 2024.
- Hiippala, T., Alikhani, M., Haverinen, J., Kalliokoski, T., Logacheva, E., Orekhova, S., Tuomainen, A., Stone, M., and Bateman, J. A. Ai2d-rst: A multimodal corpus of 1000 primary school science diagrams. *Language Resources and Evaluation*, 55:661–688, 2021.
- Hu, E. J., Shen, Y., Wallis, P., Allen-Zhu, Z., Li, Y., Wang, S., Wang, L., and Chen, W. Lora: Low-rank adaptation of large language models. *arXiv preprint arXiv:2106.09685*, 2021.
- Jiang, H., Wu, Q., , Luo, X., Li, D., Lin, C.-Y., Yang, Y., and Qiu, L. LongLLMLingua: Accelerating and enhancing LLMs in long context scenarios via prompt compression. In Ku, L.-W., Martins, A., and Srikumar, V. (eds.), *Proceedings of the 62nd Annual Meeting of the Association for Computational Linguistics (Volume 1: Long Papers)*, pp. 1658–1677, Bangkok, Thailand, August 2024. Association for Computational Linguistics. URL <https://aclanthology.org/2024.acl-long.91>.

- Khot, T., Trivedi, H., Finlayson, M., Fu, Y., Richardson, K., Clark, P., and Sabharwal, A. Decomposed prompting: A modular approach for solving complex tasks. *arXiv preprint arXiv:2210.02406*, 2022.
- Kou, S., Hu, L., He, Z., Deng, Z., and Zhang, H. Cllms: Consistency large language models. *arXiv preprint arXiv:2403.00835*, 2024.
- Lai, X., Tian, Z., Chen, Y., Li, Y., Yuan, Y., Liu, S., and Jia, J. Lisa: Reasoning segmentation via large language model. In *Proceedings of the IEEE/CVF Conference on Computer Vision and Pattern Recognition*, pp. 9579–9589, 2024.
- Li, Y., Wei, F., Zhang, C., and Zhang, H. Eagle-2: Faster inference of language models with dynamic draft trees. *arXiv preprint arXiv:2406.16858*, 2024.
- Lin, C.-Y. Rouge: A package for automatic evaluation of summaries. In *Text Summarization Branches Out*, pp. 74–81, 2004.
- Liu, A., Feng, B., Xue, B., Wang, B., Wu, B., Lu, C., Zhao, C., Deng, C., Zhang, C., Ruan, C., et al. Deepseek-v3 technical report. *arXiv preprint arXiv:2412.19437*, 2024a.
- Liu, H., Li, C., Wu, Q., and Lee, Y. J. Visual instruction tuning. *Advances in neural information processing systems*, 36, 2024b.
- Liu, Y., Li, H., Du, K., Yao, J., Cheng, Y., Huang, Y., Lu, S., Maire, M., Hoffmann, H., Holtzman, A., et al. Cachegen: Fast context loading for language model applications. *arXiv preprint arXiv:2310.07240*, 2023.
- Liu, Y., Duan, H., Zhang, Y., Li, B., Zhang, S., Zhao, W., Yuan, Y., Wang, J., He, C., Liu, Z., et al. Mmbench: Is your multi-modal model an all-around player? In *European conference on computer vision*, pp. 216–233. Springer, 2025.
- Lu, P., Bansal, H., Xia, T., Liu, J., Li, C., Hajishirzi, H., Cheng, H., Chang, K.-W., Galley, M., and Gao, J. Mathvista: Evaluating mathematical reasoning of foundation models in visual contexts. In *International Conference on Learning Representations (ICLR)*, 2024.
- Merrill, W. and Sabharwal, A. The expressive power of transformers with chain of thought. *arXiv preprint arXiv:2310.07923*, 2023.
- Meta. Introducing llama 3.1: Our most capable models to date. *blog*, 2024a. URL <https://ai.meta.com/blog/meta-llama-3-1/>.
- Meta. Llama 3.2: Revolutionizing edge ai and vision with open, customizable models. *blog*, 2024b. URL <https://ai.meta.com/blog/llama-3-2-connect-2024-vision-edge-mobile-devices>.
- Meta. torchtune: Pytorch’s finetuning library. *software*, April 2024c. URL <https://github.com/pytorch/torchtune>.
- Munkhdalai, T., Faruqui, M., and Gopal, S. Leave no context behind: Efficient infinite context transformers with infini-attention. *arXiv preprint arXiv:2404.07143*, 2024.
- Ning, X., Lin, Z., Zhou, Z., Wang, Z., Yang, H., and Wang, Y. Skeleton-of-thought: Large language models can do parallel decoding. *Proceedings ENLSP-III*, 2023.
- Papineni, K., Roukos, S., Ward, T., and Zhu, W.-J. Bleu: a method for automatic evaluation of machine translation. In *ACL*, 2002.
- Pi, R., Gao, J., Diao, S., Pan, R., Dong, H., Zhang, J., Yao, L., Han, J., Xu, H., Kong, L., et al. Detgpt: Detect what you need via reasoning. *arXiv preprint arXiv:2305.14167*, 2023.
- Qin, G., Rosset, C., Chau, E. C., Rao, N., and Van Durme, B. Nugget 2d: Dynamic contextual compression for scaling decoder-only language models. *arXiv preprint arXiv:2310.02409*, 2023.
- Radford, A. and Wu, J. Rewon child, david luan, dario amodei, and ilya sutskever. 2019. *Language models are unsupervised multitask learners*. *OpenAI blog*, 1(8):9, 2019.
- Shao, Z., Wang, P., Zhu, Q., Xu, R., Song, J., Bi, X., Zhang, H., Zhang, M., Li, Y., Wu, Y., et al. Deepseekmath: Pushing the limits of mathematical reasoning in open language models. *arXiv preprint arXiv:2402.03300*, 2024.
- Su, D., Sukhbaatar, S., Rabbat, M., Tian, Y., and Zheng, Q. Dualformer: Controllable fast and slow thinking by learning with randomized reasoning traces. *arXiv preprint arXiv:2410.09918*, 2024.
- Wang, P., Li, L., Shao, Z., Xu, R., Dai, D., Li, Y., Chen, D., Wu, Y., and Sui, Z. Math-shepherd: A label-free step-by-step verifier for llms in mathematical reasoning. *arXiv preprint arXiv:2312.08935*, 2023.
- Wei, J., Wang, X., Schuurmans, D., Bosma, M., Xia, F., Chi, E., Le, Q. V., Zhou, D., et al. Chain-of-thought prompting elicits reasoning in large language models. *Advances in neural information processing systems*, 35:24824–24837, 2022.

- Xie, Y., Kawaguchi, K., Zhao, Y., Zhao, J. X., Kan, M.-Y., He, J., and Xie, M. Self-evaluation guided beam search for reasoning. *Advances in Neural Information Processing Systems*, 36, 2024.
- Xu, G., Jin, P., Hao, L., Song, Y., Sun, L., and Yuan, L. Llava-o1: Let vision language models reason step-by-step. *arXiv preprint arXiv:2411.10440*, 2024.
- Yan, C., Wang, H., Yan, S., Jiang, X., Hu, Y., Kang, G., Xie, W., and Gavves, E. Visa: Reasoning video object segmentation via large language models. *arXiv preprint arXiv:2407.11325*, 2024.
- Yang, S., Gribovskaya, E., Kassner, N., Geva, M., and Riedel, S. Do large language models latently perform multi-hop reasoning? *arXiv preprint arXiv:2402.16837*, 2024.
- Yu, L., Jiang, W., Shi, H., Yu, J., Liu, Z., Zhang, Y., Kwok, J. T., Li, Z., Weller, A., and Liu, W. Metamath: Bootstrap your own mathematical questions for large language models. *arXiv preprint arXiv:2309.12284*, 2023.
- Yu, W., Yang, Z., Li, L., Wang, J., Lin, K., Liu, Z., Wang, X., and Wang, L. Mm-vet: Evaluating large multimodal models for integrated capabilities. In *International conference on machine learning*. PMLR, 2024.
- Yue, X., Qu, X., Zhang, G., Fu, Y., Huang, W., Sun, H., Su, Y., and Chen, W. Mammoth: Building math generalist models through hybrid instruction tuning. *arXiv preprint arXiv:2309.05653*, 2023.
- Zhang, H., Liu, Z., Zhao, Y., Zheng, J., Zhuang, C., Gu, J., and Chen, G. Fast chain-of-thought: A glance of future from parallel decoding leads to answers faster. *arXiv preprint arXiv:2311.08263*, 2023.
- Zhang, T., Kishore, V., Wu, F., Weinberger, K. Q., and Artzi, Y. Bertscore: Evaluating text generation with bert. *arXiv preprint arXiv:1904.09675*, 2019.
- Zhou, D., Schärli, N., Hou, L., Wei, J., Scales, N., Wang, X., Schuurmans, D., Cui, C., Bousquet, O., Le, Q., et al. Least-to-most prompting enables complex reasoning in large language models. *arXiv preprint arXiv:2205.10625*, 2022.

A. Training Hyperparameters

We provide the hyperparameters for the progressive encoding, additional recovering, and adaptive decoding training in Table A1.

Table A1. Training hyperparameters for progressive encoding, recovering, and adaptive decoding training.

Parameter	Progressive Encoding	Recovering	Adaptive Decoding
Epoch	1	1	1
Batch Size	6	8	8
Gradient Accumulation	1	1	1
Optimizer	AdamW	AdamW	AdamW
Weight Decay	0.01	0.01	0.01
Learning Rate	1e-04	1e-05	5e-04
Learning Rate scheduler	cosine	cosine	cosine
Warmup	100	100	100
Clip Gradient Norm	1	1	1
Activation Checkpointing	TRUE	TRUE	TRUE
FSDP	TRUE	TRUE	TRUE
Bfloat16	TRUE	TRUE	TRUE

B. Additional Results

B.1. Detailed Evaluation of Decoders

We provide the detailed evaluation results for the metrics in Table A2.

Table A2. Detailed evaluation metrics for 3 decoders.

Stage	Summary	Caption	Reasoning
BLEU	15.9	12.8	11.2
METEOR	40.1	35.5	32.7
ROUGE-L	41.6	37.9	32.7
BERTScore	73.4	71.4	66.6

B.2. Detailed Ablation Study

We provide the detailed evaluation results for the ablation study for the different number of thinking tokens and different retention ratios in Table A3 and Table A4, separately.

Table A3. Detailed results for the ablation study of different number of thinking tokens.

# Token	MMSar	MMBench	MMVet	MathVista	AI2D	Hallusion	Avg. Acc.
1	49.9	72.8	43.3	43.6	77.5	60.6	58.0
2	50.3	71.4	41.4	43.1	75.6	57.3	56.5
4	49.9	71.0	42.2	39.3	75.4	59.3	56.2
8	51.1	70.4	41.0	40.9	76.7	59.9	56.7
16	49.5	72.0	40.9	40.9	76.2	61.6	56.9
32	50.2	71.1	42.9	41.6	75.2	61.8	57.1

C. Prompts for GPT-4o Evaluation

We provide the GPT-4o prompts in Algorithm 1.

Algorithm 1 GPT-4o Prompt for CoT Decoding Evaluation

Input: Image **I**, question **Q**, decoded CoT $\hat{\mathbf{C}}\mathbf{oT}$, ground truth **CoT**,
type of CoT stage **T** \in [**caption**, **summary**, **reasoning**]

Output: An integer represents the rank of similarity between $\hat{\mathbf{C}}\mathbf{oT}$ and **CoT** in [1, 5].

User: When responding to questions about an image, a deep analysis is crucial for providing accurate answers. The analysis of an image-question pair could be one of the following components:

Summary – A brief restatement or paraphrasing of the question.

Caption – A description or summary of the content of the image.

Reasoning – A logical explanation of how the answer is derived from the image and the question.

You will be provided with one of them along with the ground truth. Your task is to evaluate whether the analysis is closely aligned with the ground truth according to given image and question pair.

User: In this conversation, you will be given a generated **T** and its ground truth.

The **T** is: $\hat{\mathbf{C}}\mathbf{oT}$.

The ground truth is: **CoT**

User: Following is the given image: **I**

The corresponding question is: **Q**

User: Please rank the similarity with an integer between 1 and 5, where the larger number means the generated **T** is more close to the ground truth. Please rate the similarity on a scale from 1 to 5, where:

1: Completely unrelated.

The generated **T** and ground truth discuss entirely different themes, and there is no overlap in content, or subject matter.

Example: Ground Truth: ...; Generated **T**: ...

2: Minimally related.

The generated **T** and ground truth are tangentially connected. Only a minimum fraction of the theme or content in ground truth is mentioned in the generated **T**.

Example: Ground Truth: ...; Generated **T**: ...

3: Somewhat related but with notable discrepancies.

The generated **T** and ground truth share key elements in theme or content but exhibit clear differences in focus, description, or details. While the overall themes or settings may overlap (e.g., animals, fences, grassy area), the generated **T** introduces significant factual errors or omits important details.

Example: Ground Truth: ...; Generated **T**: ...

4: Closely related with small differences.

The generated **T** and ground truth align on the main theme and share most of the key details. However, there are minor differences in phrasing, specific details, or focus.

Example: Ground Truth: ...; Generated **T**: ...

5: Nearly identical.

The generated **T** and ground truth are highly similar, sharing nearly all content, details, and key descriptions, with only minor or negligible phrasing differences.

Example: Ground Truth: ...; Generated **T**: ...

The output should be in a json format:

```
{ "T": (Rank), "reason": ... }
```

(Rank) is the integer of the similarity rank.

"reason" stores the reason of ranking a given **T** and ground truth.

Table A4. Detailed results for the ablation study of different number of thinking tokens.

Ratio	MMSar	MMBench	MMVet	MathVista	AI2D	Hallusion	Avg. Acc.
0.1	49.1	69.7	37.2	41.3	75.9	59.1	55.4
0.2	49.7	71.5	39.4	41.2	75.3	60.0	56.2
0.3	48.1	71.9	40.6	39.9	75.3	59.4	55.8
0.4	47.9	70.3	38.6	39.2	76.3	59.7	55.3
0.5	47.2	70.1	40.5	39.5	75.2	57.6	55.0
0.6	48.4	70.9	42.0	38.8	76.6	60.5	56.2
0.7	48.7	69.8	41.1	39.0	75.4	59.7	55.6
0.8	49.9	69.3	40.9	37.2	75.3	59.4	55.3
0.9	49.2	70.5	40.1	38.4	75.7	60.1	55.7